Role of excited states in multiphoton dynamics

Bala Sundaram and Lloyd Armstrong, Jr.
Department of Physics and Astronomy, The Johns Hopkins University, Baltimore, Maryland 21218
(Received 21 December 1987)

Multiphoton ionization of hydrogen, at laser frequencies, is studied numerically using the stretched hydrogen atom Hamiltonian. In particular, the role of excited bound states in short-pulse, above-threshold ionization (ATI) is emphasized. These states are shown to play a dynamical role both in the production of the higher ATI peaks as well as in the appearance of peak substructure. A simple criterion is used to assess the importance of this process, as a function of field strength and frequency. Arguments are presented for the interpretation of ionization characteristics for short pulses which suggest important differences from that for longer pulses. The extension of these ideas to other frequency regimes is also discussed.

INTRODUCTION

Recent experiments on multiphoton ionization over a wide range of atoms, frequencies, and field strengths report departures from strictly perturbative behavior as a function of both frequency ω and field strength F. The nature of these departures has been diverse, ranging from enhanced ionization in the microwave region[1,2] to the phenomena of multiple ionization (MI) and above-threshold ionization (ATI) at higher frequencies.[3,4] There are, however, several common features of the diverse phenomena mentioned. Among these are (a) that they are all strong field effects with respect to the considered systems; (b) they all are multiphoton processes; and (c) the qualitative features, and some of the quantitative character, may be recovered by use of simple classical or statistical models.[2,5,6] This last feature is the most puzzling, as *a priori* the dynamics, with the possible exception of the microwave regime, appear to be strongly quantum mechanical in nature. We infer, therefore, that this behavior is a reflection of the mechanism involved in these diverse processes. In the microwave frequency regime the existence of a diffusive mechanism for ionization has been explored.[7] This is closely related to strong distortion of the higher excited states in the presence of the field. In this work we present arguments for the existence of analogous behavior in the laser frquency regime. In particular, we show that several aspects of the ATI phenomenon can be addressed from the perspective of a model based on these arguments.

Most of the theoretical work addressing the question of high-field ATI has focused on the effects of the high intensity laser fields on the continuum states of the atom.[8] An implicit assumption of most of these works has been that interactions within the bound states of the atom are well represented by perturbative estimates. As stressed in a recent work,[9] however, the strength of the laser field used in a typical ATI experiment is stronger than that of the binding field for most of the excited states of the atom being irradiated. Under such conditions, one can expect that the part of the multiphoton process which occurs within these highly distorted excited states will not be simply described by a perturbative calculation.

The present study is thus motivated by a model of multiphoton ionization which focuses attention on the role of the excited bound states in the ionization process. A heuristic analysis is used to propose a simple condition to be used in analyzing multiphoton experiments, which serves to emphasize this role. A picture of ATI is developed based on this model and then tested through numerical integration of the Schrödinger equation for a one-dimensional hydrogen atom interacting with a time-dependent field.

HEURISTIC ANALYSIS

To begin to build a picture of ATI we first need to establish a measure of the distortion of an excited state by the external field. One simple indicator is obtained by comparing the field-induced width of the state with the spacing to an adjacent level. When levels are sufficiently broadened so that they overlap, we speak of these levels as being strongly mixed. A justification for this nomenclature can be found in the fact that any excitation of this region of overlapping states by absorption of a photon will produce a wave function which is an admixture of all the overlapping levels. Obviously, mixing starts with the higher levels of the atom, where field-free states are closest together, and moves lower with increasing intensity of the photon field.

Multiphoton processes such as ATI which pass through a mixing region can be expected to show strong deviations from simple perturbative behavior because of the importance of higher-order shift and width processes in the mixing regime. A simple rule of thumb to determine the importance of mixing to ATI can be obtained by considering whether or not the mixing regime extends below the threshold for one-photon ionization. If it does not, one could imagine that the excitation process would simply "jump over" the mixing regime, and that a perturbative analysis would provide a reasonable description of the process. On the other hand, if the mixing regime extends more than the energy of one photon below the ionization threshold, a simple picture of the excitation pro-

cess would show it passing through the mixing regime. This would naturally lead to a situation which would not be well described by perturbation theory.

In a normal perturbative picture of ATI an electron is moved from the initial bound state to the final continuum state in a series of virtual steps. The virtual nature of these intermediate steps means that little actual population appears in the excited levels the electron transits on its way to the continuum. When the mixing region becomes important in the ATI process we would expect some qualitative changes both in the behavior of the atom and the photoelectrons. The mixed states can be thought of as providing a sort of quasicontinuum; hence excitations into this region can preserve energy and thus become real rather than virtual. This will be reflected by an increase in the population of the states in the mixed region, and a two- (or more) step process becomes important. By this we mean that population will be moved into the mixed states, where it will be temporarily "trapped" and subsequently ionized by a single-photon process which will exhibit, naturally, a linear dependence on the intensity I. In many cases, the initial step from the ground state into the mixing region will be saturated, and the total ionization process will consequently vary rather like I. Further, one would expect the photoelectron spectrum to be affected when the mixed states participate in the ionization process. As pointed out recently,[9] the probability of n conserving transitions grows rapidly as n increases. This in turn leads to the formation of Volkov-like bound states, and these states enhance the formation of high-energy photoelectron peaks. Thus increased involvement of these highly excited states should shift the continuum electron probability toward the higher-energy photoelectron peaks. Further, the saturation of the initial step, from the ground state to the mixed states, would mean that the energy conserving points in the continuum are now decided from the intermediate excited states. This could possibly lead to the recently observed substructure[10] in the ATI spectrum. In testing this picture of ATI we consider a simple Hamiltonian describing the interaction of a bound electron with a time-dependent electric field.

MODEL CHARACTERISTICS

It has been demonstrated[11–13] that a one-dimensional model of the hydrogen atom provides a simple system that reproduces a number of the effects seen by experiment. We consider the stretched hydrogen atom[13] (SHA) interacting with a spatially homogeneous field $F(t)\cos(\omega t+\varphi)$. The SHA model is based on the realization that the dipole matrix elements coupling highly excited states in the three-dimensional hydrogen display a simple pattern. This is most clearly demonstrated and interpreted in terms of the Stark states.[14] Using the parabolic quantum numbers n, n_1, n_2, and m, transition matrix elements from a state $(n,0,n-1,0)$ to $(n', n_1'=k, n'-k-1, 0)$ are well approximated by $C(\Delta n,k)n^{2-k}$. Thus for highly excited states there is a marked propensity to undergo $k=0$ transitions and thus to remain on the ladder of extreme states $(n,0,n-1,0)$. It is the extended nature of these extreme states that allows a quasi-one-dimensional description. The largest coeffi- cients for the on-ladder transitions $C(\pm1,0)$, $C(\pm2,0)$, and $C(\pm3,0)$ are 0.32, 0.11, and 0.059, respectively. It is clear, though, that this simple behavior breaks down for the lower n states and here the SHA is to be considered only as a simple "toy" Hamiltonian. In particular for the ground state, the SHA includes only one channel for excitation and ionization. However, the results from this model, though qualitative, provide insight for a more realistic theory.

Before proceeding to a description of the numerical analysis let us first define a quantity that embodies the heuristic arguments presented earlier. This means defining the one-photon and mixing thresholds in terms of the parameters of our model Hamiltonian. For simplicity, we label both of these thresholds by their associated principal quantum numbers, represented by n_1 and n_2, respectively. Using the criteria stated, for a frequency ω and field strength F,

$$n_1=(2\omega)^{-1/2}\,,\qquad n_2=(2.7F)^{+1/5}\,. \tag{1}$$

The estimate for the mixing threshold n_2 is based on a simple two-level system and requires that the one-photon Rabi width be equal to the level spacing. Ideally, in estimating n_1 and n_2, the shifts associated with the levels should be considered. Also, the criterion used for obtaining n_2 is not the most general one, as it involves the resonant one-photon Rabi width; it would be more appropriate to use the nonresonant value for the width. It should be noted that with these changes the two thresholds would become functions of both the field strength and frequency. Further, n_1 should be generalized to correspond to the first multiphoton threshold within the mixed states. For our purpose, however, the simple estimates given by (1) are adequate.

Let us now define a parameter $R=n_2/n_1$. Figure 1 shows a schematic of the energy levels for two cases of interest, at a frequency where four photons nominally ionize the atom. Figure 1(a) corresponds to $R>1$, where the mixing sets in beyond the one-photon threshold. This is the case where the mixed states are bypassed during the ionization process due to large energy defects, and a perturbative calculation would reflect the dominant contributions. In terms of external parameters, this would correspond to very low fields or to low fields and high frequencies. Figure 1(b) shows the case $R\leq1$. Here the mixed states are levels that are important to the ionization process and nonresonant, perturbative estimates would not reflect their contributions. This occurs for very strong fields or moderate fields and low frequencies. To reiterate, the possible implications of involving the mixed states in the ionization process are the following.

(a) Population is driven into a large number of the higher excited states.

(b) Over some time scale, there is a likelihood of population being trapped in these states.

(c) The subsequent ionization of these states provides another mechanism to access the continuum. The ioniza-

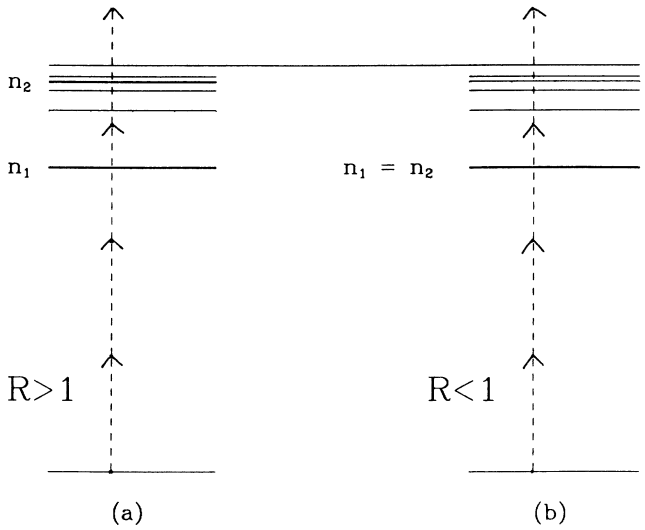

FIG. 1. Schematic of the hydrogen atom for the parametric regions (a) $R > 1$ and (b) $R \leq 1$. n_1 is the one-photon threshold and n_2 the mixing threshold.

tion process, either through absorption of a photon or tunneling, would alter the final electron spectrum.

It should be stressed that the variable R and the transition through $R=1$ merely indicate the onset of the effects described. Further characterization of the mixing would be necessary to assign a more quantitative role to this parameter. This is further complicated by the fact that the pulse profile introduces other factors relevant in determining, fully, the effects of the two thresholds.

In the dipole approximation, the considered one-dimensional Hamiltonian (in atomic units) is

$$H=\frac{p^2}{2}-\frac{1}{x}+F(t)\cos(\omega t+\varphi)x, \quad x>0 \ .$$

The time-dependent solution Φ is expressed in terms of the unperturbed basis to be

$$\Phi(t)=\sum_{n=1}^{\infty} a_n(t)\Psi_n e^{-iE_n t}+\int_0^{\infty} dk\, a_k(t)\Psi_k e^{-iE_k t} \ , \tag{2}$$

where Ψ_i are the unperturbed wave functions and a_i represent the expansion coefficients. Using (2) in the Schrödinger equation leads to a set of coupled equations for the expansion coefficients given by

$$i\dot{a}_n(t)=\sum_m Z_{nm}(t)a_m(t)+\int_0^{\infty} dk\, Z_{nk}(t)a_k(t) \ , \tag{3a}$$

$$i\dot{a}_k(t)=\sum_m Z_{km}(t)a_m(t)+\int_0^{\infty} d\kappa\, Z_{k\kappa}(t)a_\kappa(t) \ , \tag{3b}$$

where Z_{ij} denote the coupling matrix elements. The primary problem in solving (3) is in choosing an appropriate representation of the continuum. We employ a discretized continuum, also referred to as pseudodiscrete states.[15,16] This allows the terms involving the continuum to be simplified as

$$\int_0^{\infty} dk\, Z_{nk}a_k \simeq \sum_{j=0}^{n_c}\int_{k_j-\Delta_j/2}^{k_j+\Delta_j/2} dk\, Z_{nk}a_k \simeq \sum_{j=0}^{n_c} Z_{nk_j}a_{k_j}\Delta_j \ , \tag{4}$$

where k_j and Δ_j are the center and width of the jth interval and n_c denotes the number of pseudodiscrete states considered. To obtain (4) the implicit assumption is that the integrand is almost constant over the interval Δ_j. Using (4) in (3) for the bound-free and free-free terms leads to a single set of coupled differential equations

$$i\dot{y}_j(t)=\sum_{l=1}^{n_b+n_c} e^{i\omega_{jl}t}Z_{jl}(t)y_l(t) \ , \tag{5}$$

where for bound states

$$y_i=a_i$$

and for continuum states

$$y_i=\Delta_i^{1/2}a_{k_i} \ .$$

n_b is the number of bound states included and ω_{jl} is the energy difference between levels j and l. Choosing all the width Δ_i to be equal to, say, Δ, is equivalent to putting the system in a box of length $(\Delta)^{-1}$. The matrix elements for this system are known[16] and the coupled equations were solved numerically. For reasons of numerical tractability, however, it is easier to work with the $\mathbf{p}\cdot\mathbf{A}$ form of the interaction, retaining the $\mathbf{A}^2$ term as well. This is due to the relative sizes of the bound-bound, bound-free and free-free matrix elements. With $\mathbf{r}\cdot\mathbf{E}$, the free-free matrix elements, for k near k', are much larger than the others leading to possible stiff differential equations. This is eliminated in the $\mathbf{p}\cdot\mathbf{A}$ construction.

As stressed in a recent paper,[17] the interpretation of the expansion coefficients y_i as probability amplitudes is gauge dependent. We account for this by considering a shaped pulse in most of the cases presented, such that $E(t)$ and $A(t)$ are simultaneously zero, both initially and at the time of the final measurement. We do include, for comparison, square pulses which are treated under the condition that $A(t)$ is zero at both the initial and final times. It should be mentioned that from our calculations the features are not seen to be gauge dependent.

RESULTS AND DISCUSSION

Before discussing the results, the limitations of this simple treatment should be clearly stated. They are that (a) the results are affected by the size of the basis considered as well as the density of pseudodiscrete states; (b) consequently, the procedure fails for long times, though this can be controlled by the choice of Δ, the spacing of states in the continuum. For the calculations reported, the choice of basis size and total interaction time are such that these limitations do not affect the conclusions. We also verify that the appropriate low-field limits are reproduced by our calculations. Comparison of ionization rates using the SHA model with those for a more realistic, three-dimensional, treatment[18] show a consistent discrepancy of less than an order of magnitude. This is cited more to provide a perspective for our calculations rather than for any quantitative assessment.

We considered a wide range of frequencies and field strengths in our computations. However, we present our

arguments by considering only a few representative cases. Figure 2 shows the ionized fraction as well as the trapped fraction as a function of intensity, for a typical case. The intensity range considered is 10^{-6}–4×10^{-3} a.u. corresponding to, roughly, 7×10^{10}–3×10^{14} W/cm^2, and the photon frequency is 0.148 a.u. (nominally, four-photon ionization). The trapped fraction is defined as the population in states labeled by quantum numbers $n \geq n_2$, where n_2 is given by Eq. (1). The field profile is a square pulse with a duration of 50 fs. A basis of 40 bound states and 100 continuum states was used in this calculation.

A useful indicator of the intensity dependence of multiphoton ionization is an index k defined in terms of the total or partial ionization rate P and intensity I as

$$k = \frac{d \ln P}{d \ln I} .$$

k is commonly referred to as the effective order of nonlinearity. In this case, ionization involves a minimum of four photons and lowest-order perturbation theory (LOPT) would thus predict a value of 4 for k. The ionization curve in Fig. 2 shows three distinct regimes characterized by differing slopes. At the lower intensities (less than 10^{-4}), the slope is approximately 1 changing with increasing intensity to approximately 4 and, finally, to about 1.25. The discrepancy, at low intensities, between the measured slope and the LOPT prediction is a consequence of the short interaction time considered in our calculation. For short times the rate regime is not attained and the ionized fraction shows rapid oscillations[19] in time. This portion of the curve has been included primarily for completeness rather than for any predictive value. With increasing intensity, the rate regime is achieved within the time considered and the LOPT result is seen. Further increase in intensity saturates this transition rate. The intensity at which k becomes approximately linear (1.25 in this case) is referred to as the saturation intensity.

As seen from the upper axis, increasing intensity corresponds to $R \rightarrow 1$ and at an intensity of 1.6×10^{-3} a.u., R is equal to 1.2. The relationship between decreasing values of R and the change in slope is consistent with earlier predictions. As stressed earlier the relationship is a qualitative one which is seen at all the other frequency values considered.

Figure 3 illustrates the intensity dependence of the ionized and trapped fractions at a lower frequency of 0.09 a.u. In this case a minimum of six photons are required for ionization. The lower photon energy requires increased resolution in the continuum and a basis of 30 bound and 240 continuum states was used. Further, the pulse was shaped by a $\sin^2(\pi t/2t_s)$ envelope function where $2t_s$, the total pulse duration, was taken to be 50 fs. The range of intensities considered is narrower than for Fig. 2. For the ionized fraction, the index k follows the same pattern, varying from a value (approximately equal

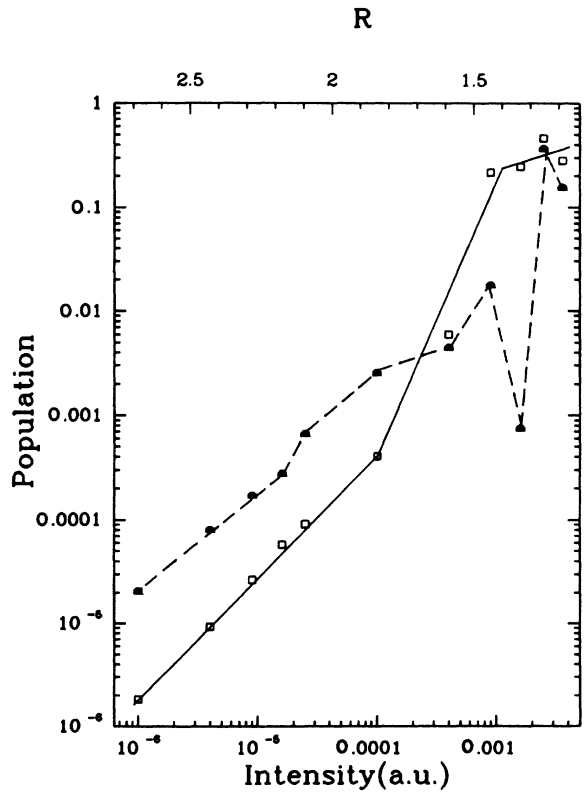

FIG. 2. Fractional population as a function of intensity (in a.u.) at a frequency 0.148 a.u. The solid curve shows the ionized fraction while the dashed curve is population in states above the mixing threshold.

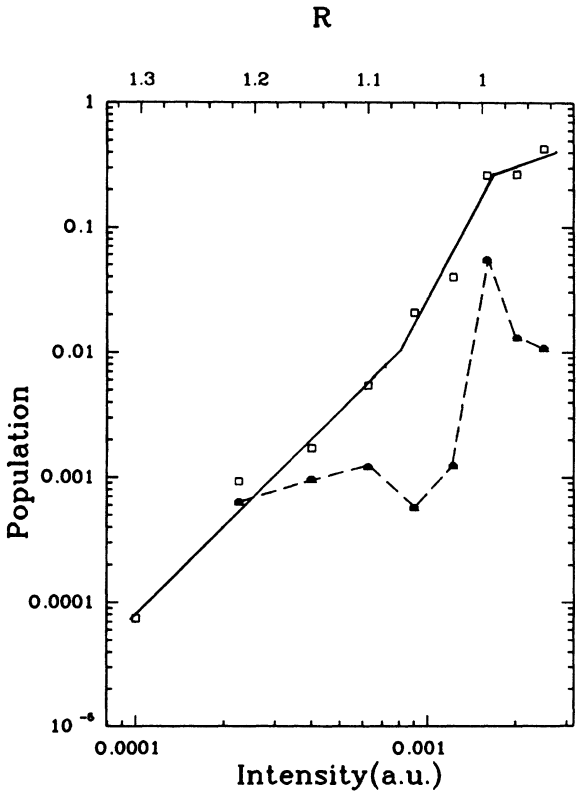

FIG. 3. Same as in Fig. 2 at a frequency 0.09 a.u. with the ionized fraction (solid line) and trapped fraction (dashes). Note that a shaped pulse with a total duration of 50 fs was used for the calculations.

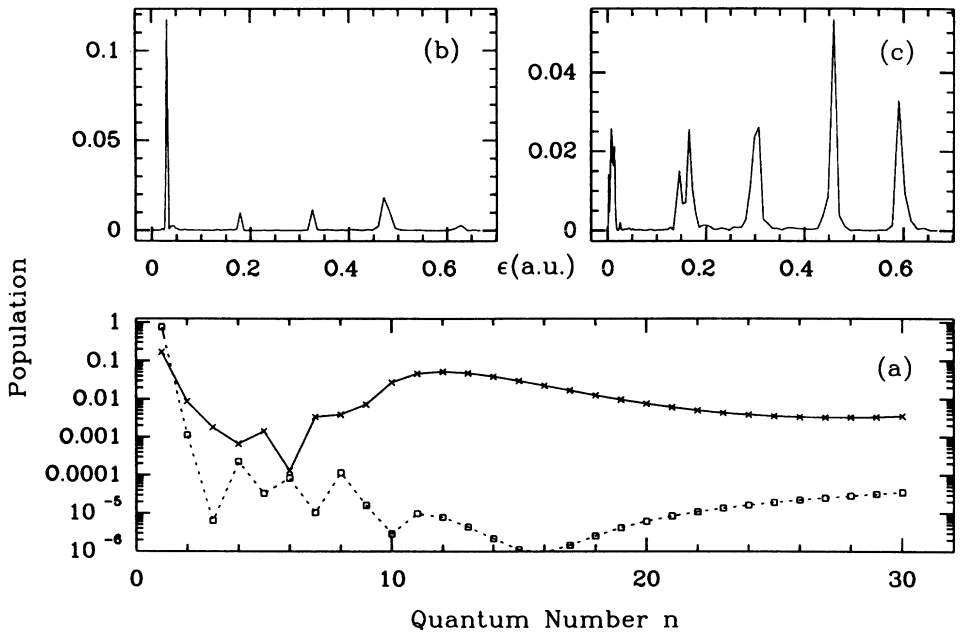

FIG. 4. (a) Population in the first 30 bound states, labeled by the principal quantum number n. The solid curve is at an intensity of 2.5×10^{-3} a.u. while the dashed curve corresponds to an intensity of 1.6×10^{-3} a.u. (b) and (c) The continuum population as a function of energy (a.u.) at (b) 1.6×10^{-3} a.u. and (c) 2.5×10^{-3} a.u. Frequency $\omega=0.148$ a.u.

to 2.5) below the LOPT prediction of 6 through the LOPT region to a value of approximately 1.1. The index R is close to 1.0 at an intensity of 1.6×10^{-3} a.u. and correlates well with the change to quasilinear slope.

A striking feature at both frequencies is the population remaining in the bound states even at intensities above the saturation value. This high intensity regime is of interest because the normal interpretation associates the transition to linear slope with the total depletion of neutral atoms. The presence of the trapped population, however, suggests a need to alter this definition for the case of short pulses.

Having ascertained the gross characteristics, let us now examine these features more closely by considering a few cases in detail. Figures 4(b) and 4(c) show the fractional population in the continuum as a function of electron energy at $\omega=0.148$ a.u. Figure 4(b) is at an intensity of 1.6×10^{-4} a.u. while for Fig. 4(c) the intensity is

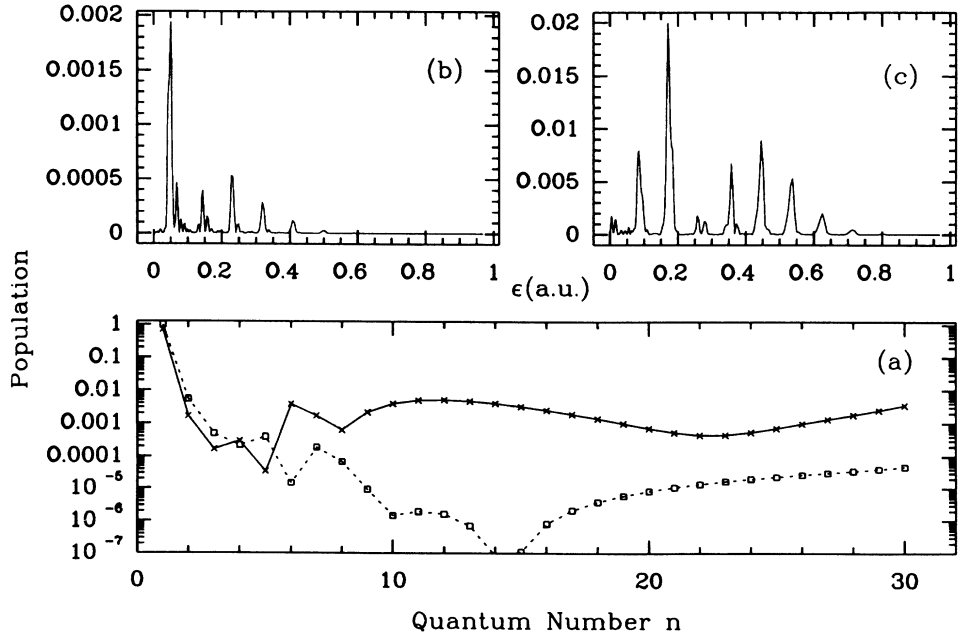

FIG. 5. Same as Fig. 4 at a frequency of 0.09 a.u. with a shaped pulse. (a) The solid curve is at an intensity of 1.6×10^{-3} a.u. while the dashed curve corresponds to an intensity of 9.0×10^{-4} a.u. (b) and (c) The continuum population as a function of energy (a.u.) at (b) 9.0×10^{-4} a.u. and (c) 1.6×10^{-3} a.u.

2.5×10^{-4} a.u. Both intensities are in the region defined by $k\sim1$. The pulse profile is, as for Fig. 2, a 50-fs square pulse. The ATI peaks are clearly defined at the higher intensity whereas, at the lower intensity, the lowest-order peak is the only one that is well resolved. Figure 4(a) shows the population in the first 30 bound states, as a function of the principal quantum number n, for the two intensity values. It is clear that significant population is driven up into the excited states at the higher intensity value. It should be noted that at a frequency of 0.148 a.u. the $n=1$ and $n=3$ states are near resonant with three photons. Therefore one would expect the population in the $n=3$ state to be resonantly enhanced. However, as mentioned earlier, the mixing threshold in this case is also the state $n=3$. This means that the higher excited states are populated at a rate comparable to the $n=3$ state, accounting for the absence of any resonance structure. Figure 5 shows similar behavior at a frequency of 0.09 a.u. In this case a 50-fs shaped pulse was used. Figures 5(b) and 5(c) correspond to $R>1$ and <1, respectively. The increase in the trapped population at the higher field value is in agreement with earlier predictions based on the relative positions of the two thresholds.

The role of R is emphasized in Table I, which compares the ionized and trapped fraction for several frequencies at a fixed intensity of 1.6×10^{-3} a.u. The total interaction time is also held fixed. The ratio of trapped to ionized population P_{ti} is shown in the last column. Our simple estimate for parameter R is a qualitative measure of the relative importance of processes involving the mixed states to ones that bypass them. As emphasized earlier, this does not include the field profile characteristics which are relevant for determining the ionized and trapped fractions. Further, excitation of the mixed states proceeds through the first excited state. For fixed field strength, the effective rate for this first step drops off with decreasing ω. Therefore, given the constant interaction time, the depletion of the ground state is strongly frequency dependent. The ratio P_{ti} normalizes the results at different frequencies and is a better measure of the competing processes. Thus the efficacy of R is better judged by this ratio. The equivalence of the two quantities is clearly seen in Table I.

The case of $\omega=0.2$ is striking, as it does not follow the pattern established by the other frequency values shown. The reason for this is useful to establish as it is exploited for a subsequent result. At this frequency there is a near resonance between the states $n=1$ and 2. The mixing regime starts from $n=3$ and the one-photon threshold is at $n=2$. Thus the near resonance provides a mechanism

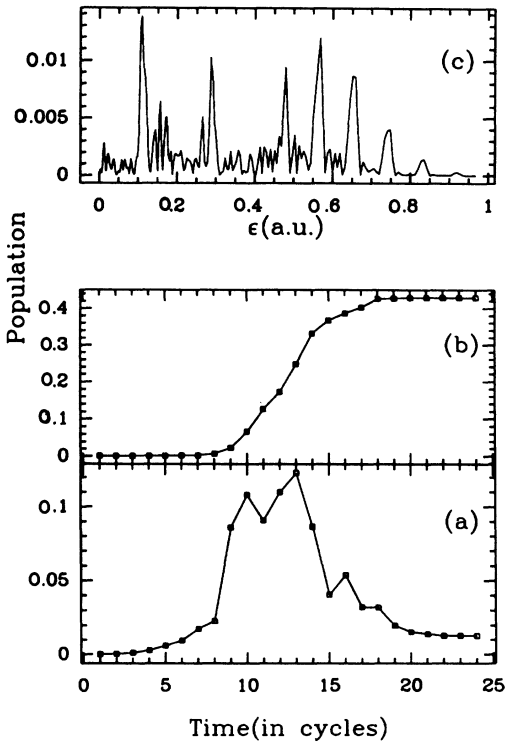

FIG. 6. (a) Excited-state fraction and (b) ionized fraction as a function of time. $\omega=0.09$; $F_0=0.5$; $\sin^2(t/\tau_s)$ pulse. (c) Electron spectrum as a function of energy at the end of the pulse (50 fs).

for jumping over the mixed states and diminishing their contribution to the ionization process. This mechanism is used later in studying the role of the mixed states in producing substructure in the ATI peaks.

In establishing the contribution of excited states in the ionization and ATI processes we have assigned a purely static role to the indicator R. The need to assign a dynamical role is motivated by the observation in recent experiments on ATI, with short-time pulses,[10] of substructure in the peaks. This substructure, within the individiual ATI peaks, is also seen in both Figs. 4 and 5. Further, the development of ATI structure is seen to correlate well with the increase in population in the excited levels. This would suggest that the excited states may play a crucial role in understanding the ATI phenomenon as all as peak substructure. To pursue this notion we need to explore the ionization mechanism in more detail. We address this question by looking at three different aspects of the problem: (1) the time dependence of the ex-

TABLE I. Trapped and ionized fractions as a function of frequency for fixed field $F_0=0.04$ a.u. N is the minimum number of photons required for ionization.

ω (a.u.)	R	N	P_i (ionized)	P_t (trapped)	$P_{ti}=P_t/P_i$
0.3	1.8	2	2.39×10^{-1}	7.87×10^{-8}	2.3×10^{-7}
0.2	1.47	3	7.96×10^{-1}	3.94×10^{-8}	0.5×10^{-7}
0.148	1.26	4	1.22×10^{-1}	1.87×10^{-4}	1.5×10^{-3}
0.09	0.94	6	4.29×10^{-1}	1.05×10^{-2}	2.4×10^{-2}
0.046	0.70	11	1.16×10^{-1}	6.31×10^{-3}	5.4×10^{-2}

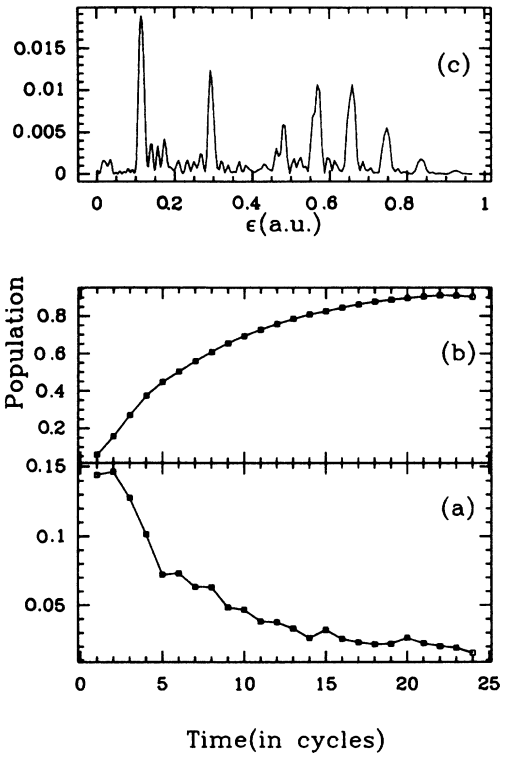

FIG. 7. Same as Fig. 6 but for a square pulse.

cited and ionized fractions, (2) the role of intermediate resonances in creating the peak substructure, and (3) the electron spectrum produced from excited states above and below the mixing threshold.

Figures 6(a) and 6(b) show the excited state and ionized populations as a function of time, measured in cycles of the external field. A frequency of 0.09 (six-photon ionization) and a shaped pulse of peak field strength 0.05 a.u. are considered. The pulse duration is 24 cycles ($\sim$50 fs). Ionization sets in at a critical field which, in keeping with earlier analysis,[20] is found to be independent of the pulse duration. With rising field there is simultaneous increase in both ionized and excited population. The excited-state population exhibits several peaks which reflect the competing processes of depletion through ionization and excitation from the ground state. We have verified that the oscillation in the excited-state population is not related to fluctuations of the ground-state population but is a consequence of ionization. Figure 6(c) shows the electron spectrum at the end of the pulse. The spectrum is seen to be noisy, particularly for low energies. Indications of the origins of this behavior can be found on comparison with Figs. 7, which show analogous plots for a square pulse. In this case initial transients are seen to drive population into the excited states which decay rapidly into the continuum. The electron spectrum shows better defined ATI peaks, without much of the substructure seen in the case of the shaped pulse. A possible explanation of the

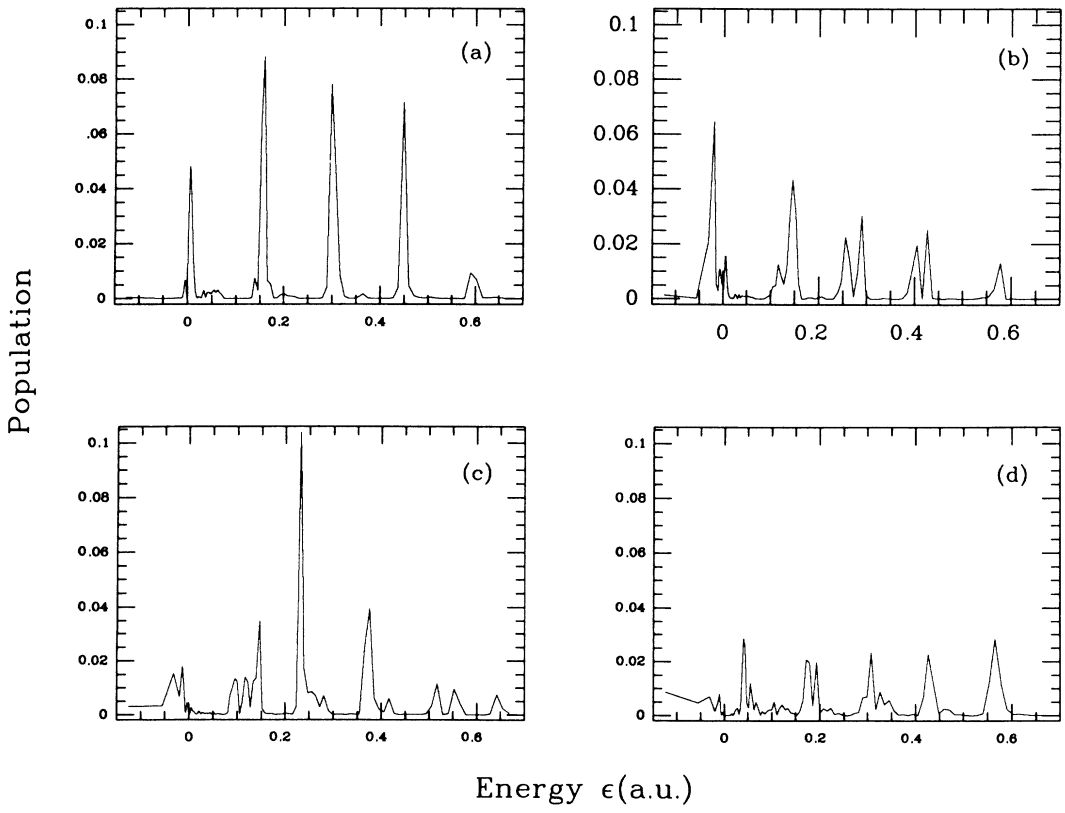

FIG. 8. Fractional population as a function of energy (a.u.) for (a) $\omega=0.148$, (b) $\omega=0.142$, (c) $\omega=0.138$, (d) $\omega=0.130$; ω is the frequency in a.u. For all cases the intensity is 2.5×10^{-4} a.u.

differences is based on the role of dynamical shifts and widths in the case of the shaped pulse. These would bring different higher excited states into resonance as a function of time. The subsequent decay of these state would produce satellite ATI peaks which would constitute the substructure. The "static" atomic spectrum associated with the square pulse would discount such a mechanism. If this were the process the field profile would play an important role in the electron spectrum, at least for short pulses. For longer pulses this would not be a factor especially if all the atoms are fully ionized before the peak field is attained. Further, with this picture, tuning the frequency to be resonant with one of the lower excited states would inhibit the substructure. This is what was seen in Table I for $\omega=0.2$ where passage through the mixed states was diminished by the presence of a near resonance with a lower excited state.

In our numerical experiments this picture can be easily demonstrated. Figure 8 shows the fractional population as a function of energy at four values of the frequency. The intensity is 2.5×10^{-4} a.u. and the pulse envelope $\sin^2(\pi t/2t_S)$ is used; all four frequencies correspond to nominal four photon ionization. Figure 8(a) is at the frequency (0.148 a.u.) near resonant for a three-photon transition between $n=1$ and $n=3$; Figs. 8(b)–8(d) display a sequence increasingly detuned from this resonance. The development of substructure within the ATI peaks is seen to correlate with the increasing detuning. Preliminary analysis indicates that a simple two-state diagonalization, involving $n=2$ and $n=3$, is inadequate to resolve the structure. It would appear, as anticipated, that for the nonresonant cases there are several states that are dynamically drawn into resonance and contribute to the ionization. In Fig. 8(a), the near-resonance case, the dominant mechanism is through the $n=3$ state. In Fig. 8(b) a prominent peak is seen within the negative energy states. This is not a "subthreshold peak"[12] but corresonds to population centered around the $n=5$ state.

The multilevel nature of the process is stressed in Fig. 9, where electron spectra arising from different approximations are compared. Figure 9(a) is the spectrum obtained on retaining all the bound and continuum couplings. In Fig. 9(b) the continuum-continuum coupling is not included. The overall ionized fraction remains constant though the distribution in energy is quite different. Figure 9(c) is motivated by the Volkov state approximation[21] and has a single bound state coupled to the continuum. For the interaction times we considered (50–100 fs) the spectra had not developed fully in this approximation but the rates are seen to be several orders of magnitude lower. From our perspective, the short-pulse intense field regime is characterized by competing rates and associated time scales which require inclusion of all possible couplings. It it, therefore, highly unlikely that approximations that neglect part of the spectrum would be very successful.

Further information on the electron spectrum may be had from looking at ionization from the excited states. This is relevant not only to the question of substructure but to the origin of the ATI phenomenon. Figures (10) and (11) show the population distribution in both bound and continuum states for a range of initial states. The

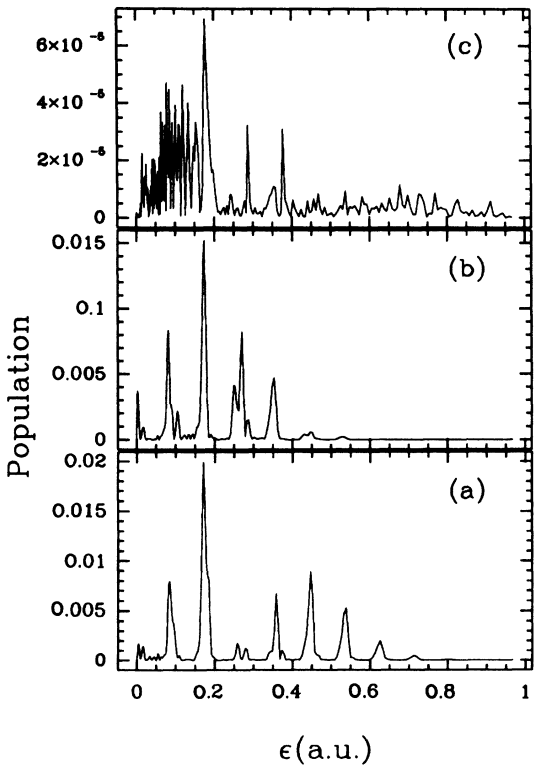

FIG. 9. Distribution of electrons as a function of energy ϵ. $\omega=0.09$ a.u., $F=0.04$, and $n_0=1$. (a) 30 bound states; (b) 30 bound states, no continuum-continuum coupling; (c) one bound state. (a) and (b) use a shaped pulse while (c) is for a square pulse.

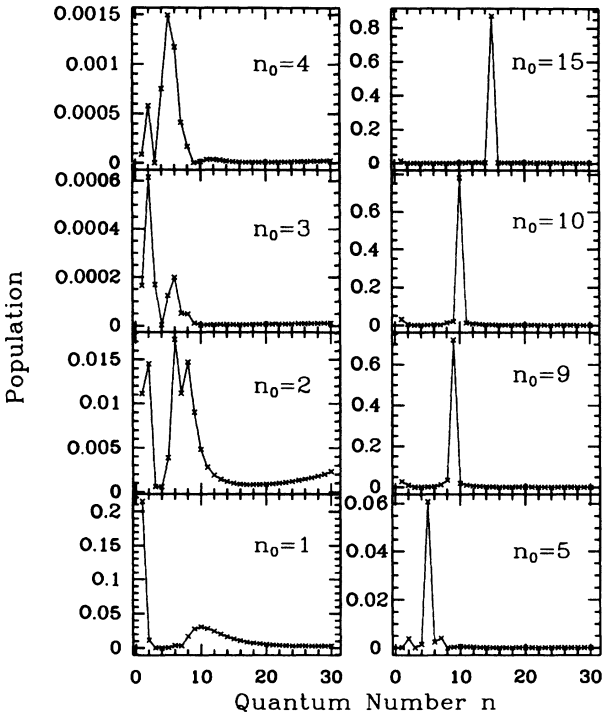

FIG. 10. Population distribution within the bound states $\omega=0.148$, $F=0.05$ for different initial states n_0 for a shaped pulse of duration 20 cycles (approximately 25 fs).

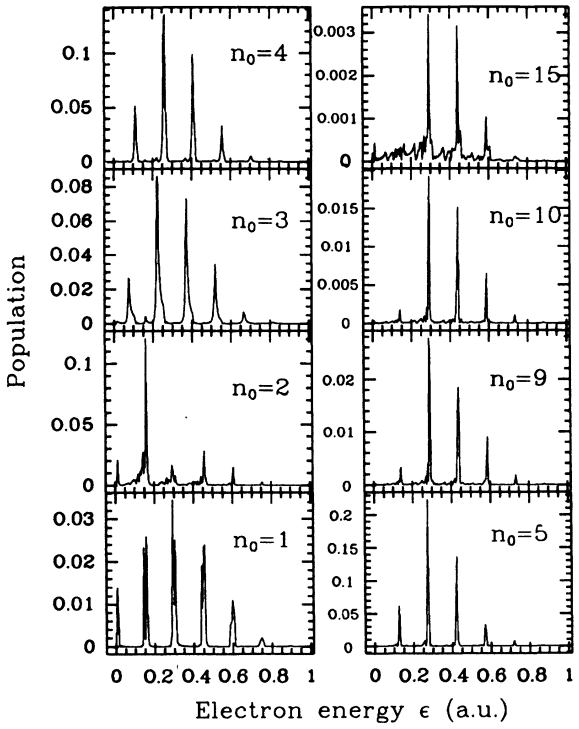

FIG. 11. Electron spectra for the same conditions as Fig. 10.

field parameters are a frequency of 0.148 and field strength of 0.05, which puts the mixing threshold at $n=3$ and $R\sim 1.2$. Thus initial states $n\geq 2$ are also within the one-photon threshold. The highly localized bound state distributions, for states above the mixing threshold, is distinctive as is the similarity in their corresponding electron spectra. Though all the features are not fully understood we suggest that they manifest the increasing importance of diagonal couplings both within the bound and continuum states. These could be introduced by "dressing" the bare atomic states. The major feature of dressing is that it isolates the diagonal couplings. This has to be done consistently for both bound[9] and continuum[22] states. Just treating the bound states would give the probability of populating the sth peak P_s, from within the one-photon threshold, to be

$$P_s \propto J_s^2(\lambda_b)\,|\,V_{bE}\,|^2\,,$$

where $\lambda_b=\frac{3}{2}n(n-1)F/\omega$, V_{bE} is a bound-free matrix element and J_s is a Bessel function of the first kind. This is valid in the absence of continuum-continuum coupling. Including dressed continuum states[22] in a simple first-order calculation yields a dependence on a combination of J_{s-1}, J_s, and J_{s+1} which does not fully reproduce the results obtained. However, our preliminary analysis indicates that this may be a reasonable way to treat states within the mixed regime. Work is in progress to address this issue further.

CONCLUSIONS

We have shown, through the use of a simple model, that the smearing out of part of the discrete spectrum of an atom, when interacting with a strong laser field, may be responsible for many of the features seen in recent multiphoton experiments. The fact that this can be either in the lower excited states or the Rydberg sequence allows the extension of these ideas to other frequency and field regimes. For the hydrogen atom, laser frequencies and intensities allow only a nominal range of variance for a parameter such as R. It is also clear that at extreme frequencies the parameter R is restricted only to one regime. Going to the Rydberg sequence with the use of microwaves appears to be the other extreme of limited variability. In that case mixing is the dominant feature[2] and is seen as the reason for the success of classical modeling.[11] Infrared frequencies are ideal for exploring a wider range of the parameter R, and this idea is projected for a subsequent publication.

The model presented can also be modified to address the question of "localization" effects[7] seen in the excitation and ionization of highly excited hydrogen atoms by microwaves. These have been interpreted as quantum-mechanical features that inhibit a classical, diffusive, ionization mechanism and become more relevant, at fixed field strength, with increasing frequency. At these higher frequencies, the mechanism of jumping over part of the mixed regime becomes more important. This would reassert the discrete nature of the spectrum and could serve to curtail the diffusive behavior. This is a scenario that is currently being explored.

In summary, our primary conclusions are the following.

(a) The two-threshold characterization of the bound states allows a consistent treatment of strong-field ionization.

(b) The excited levels play an active dynamical role in the above-threshold ionization process. This would suggest that the use of effective matrix elements is inadequate to represent the process.

(c) The mixing of excited levels could be a possible explanation for substructure in the ATI peaks as well as the anomalous effective orders of nonlinearity observed[3] for the electron spectrum. This, in conjunction with dynamical role assigned to the excited states, would enhance the importance of the field profile in describing short-pulse ATI.

(d) The concept of saturation intensity as the point of total depletion of the neutral atoms may have to be redefined for short-pulse experiments.

Despite the limitations of the simple model used here, we have demonstrated that it provides a useful medium to test aspects of multiphoton dynamics. More realistic analytic and numerical calculations are under way to verify these preliminary results.

ACKNOWLEDGMENTS

This work was supported in part by a grant from the U.S. National Science Foundation. The numerical calculations were performed on a CRAY XMP at the Pittsburgh Supercomputing Center.

[1]J. E. Bayfield and L. A. Pinnaduwage, J. Phys. B **18**, L49 (1985); Phys. Rev. Lett. **54**, 313 (1985).
[2]K. A. H. van Leeuwen, G. v. Oppen, S. Renwick, J. B. Bowlin, P. M. Koch, R. V. Jensen, O. Rath, D. Richards, and J. G. Leopold, Phys. Rev. Lett. **55**, 2231 (1985).
[3]P. Kruit, J. Kimman, H. G. Muller, and M. J. van der Wiel, Phys. Rev. A **28**, 248 (1983).
[4]T. S. Luk, H. Pummer, K. Boyer, M. Shahidi, H. Egger, and C. K. Rhodes, Phys. Rev. Lett. **51**, 110 (1983).
[5]M. Crance, J. Phys. B **17**, L355 (1984); **17**, 4333 (1984).
[6]Liwen Pan, J. Phys. B **18**, L833 (1985).
[7]G. Casati, B. V. Chirikov, D. L. Shepelansky, and I. Guarneri, Phys. Rep. **154**, 77 (1987).
[8]See, *Photons and Continuum States of Atoms and Molecules,* edited by N. K. Rahman, C. Guidotti, and M. Allegrini (Springer-Verlag, Berlin, 1987).
[9]Liwen Pan, Bala Sundaram, and L. Armstrong, Jr., J. Opt. Soc. Am. B **4**, 754 (1987).
[10]R. R. Freeman, P. H. Buchsbaum, H. Milchberg, S. Darack, D. Schumacher, and M. E. Geusic, Phys. Rev. Lett. **59**, 1092 (1987).
[11]J. N. Bardsley, B. Sundaram, L. A. Pinnaduwage, and J. E. Bayfield, Phys. Rev. Lett. **56**, 1007 (1986).
[12]J. Javanainen and J. H. Eberly (unpublished).
[13]J. N. Bardsley and B. Sundaram, Phys. Rev. A **32**, 689 (1985).
[14]H. A. Bethe and E. E. Salpeter, *Quantum Mechanics of One- and Two-electron Atoms* (Springer-Verlag, Berlin, 1957).
[15]R. D. Cowan, *The Theory of Atomic Structure* (University of California, Berkeley, 1981).
[16]S. Susskind and R. V. Jensen, Phys. Rev. A (to be published).
[17]W. E. Lamb, Jr., R. R. Schlicher, and M. O. Scully, Phys. Rev. A **36**, 2763 (1987).
[18]S.I. Chu and J. Cooper, Phys. Rev. A **32**, 2769 (1985).
[19]S. L. Haan and S. Geltman, J. Phys. B **15**, 1229 (1982).
[20]P. Lambropoulos and X. Tang, J. Opt. Soc. Am. B **4**, 821 (1987).
[21]H. Reiss, Phys. Rev. A **22**, 1786 (1980); see also Ref. 8, pp. 98–103.
[22]Liwen Pan (unpublished).